Advances in Nano Research, *Vol. 4, No. 1 (2016) 1-14*
DOI: http://dx.doi.org/10.12989/anr.2016.4.1.001

Effect of additives on the hydrothermal synthesis of manganese ferrite nanoparticles

Marija Kurtinaitienė, Kęstutis Mažeika, Simonas Ramanavičius, Vidas Pakštas and Arūnas Jagminas*

State Research Institute Centre for Physical Sciences and Technology, Savanoriu 231, LT-02300 Vilnius, Lithuania

(Received June 12, 2015, Revised January 11, 2016, Accepted January 15, 2016)

Abstract. Superparamagnetic iron oxide nanoparticles (*Nps*), composed of magnetite, Fe_3O_4, or maghemite, γ-Fe_2O_3, core and biocompatible polymer shell, such as dextran or chitozan, have recently found wide applications in magnetic resonance imaging, contrast enhancement and hyperthermia therapy. For different diagnostic and therapeutic applications, current attempt is focusing on the synthesis and biomedical applications of various ferrite *Nps*, such as $CoFe_2O_4$ and $MnFe_2O_4$, differing from iron oxide *Nps* in charge, surface chemistry and magnetic properties.

This study is focused on the synthesis of manganese ferrite, $MnFe_2O_4$, *Nps* by most commonly used chemical way pursuing better control of their size, purity and magnetic properties. Co-precipitation syntheses were performed using aqueous alkaline solutions of Mn(II) and Fe(III) salts and NaOH within a wide pH range using various hydrothermal treatment regimes. Different additives, such as citric acid, cysteine, glicine, polyetylene glycol, triethanolamine, chitosan, etc., were tested on purpose to obtain good yield of pure phase and monodispersed *Nps* with average size of ≤20 nm. Transmission electron microscopy (TEM), *X*-ray diffraction, energy dispersive *X*-ray spectroscopy (EDX), Mössbauer spectroscopy down to cryogenic temperatures, magnetic measurements and inductively coupled plasma mass spectrometry were employed in this study.

Keywords: manganese ferrite; nanoparticles; hydrothermal synthesis; phase purity; magnetic properties

1. Introduction

In recent years, considerable interest has been devoted to fabrication of various ferrite nanoparticles (*Nps*) with the aim of developing the convenient method for synthesis of uniform *Nps* with predictable size, morphology and homogeneity. This need is dictated by the increasing interest in application of superparamagnetic nanoparticles and ferrofluids in catalysis, waste water treatments and nanomedicine, in particular, diagnostics, magnetic hyperthermia, drug delivery systems, etc. (Gupta and Gupta 2005, Corchero and Villaverde 2009, Laurent *et al*. 2008, Kumar and Mohammad 2011, Banerjee and Chen 2008, Latrigue *et al*. 2012). Conventional solid-state syntheses, such as ball milling (Jiang *et al*. 1999), gas phase deposition (Pratsinis and Vemury

*Corresponding author, Ph.D., E-mail: jagmin@ktl.mii.lt

http://www.techno-press.com/?journal=anr&subpage=7 ISSN: 2287-237X (Print), 2287-2388 (Online)

1996) or laser ablation cannot meet these requirements. As reported, quite monodisperse Me (Me=Co, Ni, Mn, Zn) ferrites with size distribution less than 15% can be obtained by high temperature induced decomposition/oxidation of organic precursors, such as Me acetylacetonates and Me carbonyls in high-boiling organic solutions with surfactants (Sun *et al.* 2004, Zeng *et al.* 2004). Note that in the latter case, obtained *Nps* are soluble only in organic solvents. Re-dispersion of these *Nps* in aqueous solutions is cost-effective and time-consuming process resulting in the significant increase of *Nps* hydrodinamic size and modification of magnetic core properties. Therefore, other solution-based syntheses of various ferrites by co-precipitation route from alkaline solutions of corresponding Me(II) and Fe (III) salts are frequently being considered as more promising due to no need of hazardous Me precursors, solvents and surfactants as well as one-pot synthesis way (Mahmoudi *et al*. 2011). In this field, perhaps, the most remarkable progress has been made by convenient hydrothermal or micro wave-assisted co-precipitation using Fe(III) and Fe(II), Co(II), Zn(II), Ni(II) or Mn(II) alkaline solutions (Tourinho *et al*. 1990, Ahn *et al.* 2012; Pereira *et al*. 2012). It is of note, that currently more than 83 % of superparamagnetic *Nps* are fabricated by chemical methods, among which more than 51 % is ascribed to co-precipitation approach (Mahmoudi *et al*. 2011). However, the synthesis of pure phase, stoichiometric and uniformly-sized $MeFe_2O_4$ *Nps* still remains a serious challenge (Laurent *et al*. 2008, Salazar *et al*. 2011). Moreover, the physical and chemical properties of the obtained magnetic *Nps* are strongly dependent on the synthesis conditions, such as precursors and alkali nature, pH and synthesis regime (Lu *et al*. 2007, Pereira *et al.* 2012).

Among other ferrites, manganese ferrite, $MnFe_2O_4$, is a soft spinel-type material with high magnetic permeability and its thermal stability (Janghorban and Shokrollahi 2007, Shokrollahi 2008), as well as high magnetization and relaxation, making *Nps* of this material especially suitable for hyperthermia treatment (Yang *et al*. 2010). In the past two decades, solvothermal (Solano *et al*. 2012), hydrothermal (Bao *et al*. 2009), Langmuir-Blodgett (Lee *et al.* 2005), sol-gel (Pramanik *et al*. 2004), ball milling (Liu *et al*. 2006) and bacteria-initiated (Coker *et al*. 2009) approaches, among others, have already been suggested for fabrication of cobalt and manganese ferrite *Nps* differing in size, crystallinity and saturation magnetization ranging between 58.7 and 79 emu/g. It the case of solvothermal synthesis in alkaline ethylene glycol solution, however, it has been demonstrated that the composition of the final product depends on the content of alkali used, whereas decrease in the pH leads to the formation of Fe_2O_3 and Mn_3O_4 mixture instead of $MnFe_2O_4$ (Pereira *et al*. 2012). This effect was linked with the influence of OH^- ions, which stabilize further growth of the as-formed $MnFe_2O_4$ crystallites. We note that to enhance the uniformity of *Nps*, various surfactants and complexants such as structure-modifying agents, which inhibit growth of *Nps*, are frequently used, especially in the hydrothermal reactions (Bao *et al*. 2009). At the same time, we found recently that in the case of $MnFe_2O_4$ synthesis, the application of common co-precipitation principles may result in the formation of non-stoichiometric *Nps* with a low yield. However, the effect of such traditional additives as citrates, amino acids and polymers, which are known to influence the growth of other *Nps*, on the purity, composition and yield of manganese ferrite *Nps* was not investigated in detail until now. To the best of our knowledge, this is the first report on the peculiarities of $MnFe_2O_4$ *Nps* formation by hydrothermal approach using various structure-modifiers such as surfactants (polyethylene and polypropylene glycols), complexants (citric and tartaric acids, their salts), amino acids moieties (cysteine, glycine) and carbohydrates (glucose, chitosan, etc) at various concentrations and solution pHs. The composition of obtained products, their morphology, yield and magnetic properties were studied. We believe that this work sheds new light on the design of $MnFe_2O_4$ *Nps* with improved purity, yield and

monodispersity. High resolution transmission electron microscopy, *X*-ray diffraction, inductively coupled plasma-assisted emission analysis, Mössbauer spectroscopy and magnetometry measurements were performed.

2. Experimental

2.1 Materials

All reagents in this study were of analytical grade, at least, and used without any further purification, with the exception of NaOH. $MnSO_4 \cdot 5H_2O$, $Fe_2(SO_4)_3 \cdot 5H_2O$, $MnCl_2 \cdot 4H_2O$, $FeCl_3 \cdot 6H_2O$, citric, diglycolic and tartaric acids, their salts and glucose were purchased from Aldrich Chemicals Inc. (USA). L-cysteine and glycine were purchased from ROANAL (Hungary). Polyethylene glycol 3000 (PEG-3000), polypropylene glycol 425(PEG-425) and chitosan were purchased from ALDRICH Chemistry (Germany). Triethalolamine (pure grade) was obtained from FIRMA CHEMPUR (Poland), whereas NaOH was purchased from Poch SA (Poland) and purified by preparing of saturated solution, what resulted in the crystallization of others sodium salts. Deionised distilled water was used throughout all experiments.

2.2 Synthesis of Mn-ferrite nanoparticles

In this study, Mn-ferrite *Nps* were synthesized using alkaline solutions of Mn(II) and Fe(III) salts and NaOH in the Teflon-lined stainless steel autoclave with 25 mL volume, and in the microwave borosilicate glass reactor with 30 mL volume (ANTON Paar Microwave synthesis reactor, Monowave 300) by co-precipitation method at 110° to 140℃ for up to 15 h. The working solutions were prepared from either $MnCl_2 \cdot 4H_2O$ and $FeCl_3 \cdot 6H_2O$ or $MnSO_4 \cdot 5H_2O$ and $Fe_2(SO_4)_3 \cdot 5H_2O$ salts. Various complexing and chelating agents for Mn(II) and Fe(III) ions were also tested. In all the cases total concentration of metal salt was ≤100 mmol/L. In order to obtain stoichiometric composition of *Nps*, the initial mole concentration of Mn(II) and Fe(III) salts in the reaction medium was set at 1:2. All solutions were deoxygenated with argon before mixing. The pH of solutions was adjusted by addition of 5.0 mol/L NaOH solution to range between 9.0 and 13.0. The required quantity of NaOH solution in each case was determined by additional blank experiment. In the subsequent experiment, this quantity was added to the reactor and mixed with all other components by means of vigorous stirring for several seconds. The as-grown products were collected by centrifugation at 8500 rpm for 3 to 9 min and carefully rinsed 5 times using new portions (10 mL) of H_2O and, finally, ethanol. The precipitated products were dried at ~60℃ overnight and used in further processing within the following week.

2.3 Analysis

The stoichiometry of synthesized $MnFe_2O_4$ Nps was analyzed by means of inductively coupled plasma mass spectrometry. Nps were dissolved in HCl (1:1) and the contents of manganese and iron were analyzed. Measurements were made on emission peaks at λ_{Mn}=257.610 nm λ_{Mn}=259.372 nm and λ_{Fe}=238.204 nm using a OPTIMA 7000DV (Perkin Elmer, USA) spectrometer. Calibration curves were made using dissolved standards within 1 to 50 ppm concentrations in the same acid matrix as the unknowns. Standards and unknowns were analyzed at least 5 times. The

detection limits based on three standard deviations result in ±3.5% error. All standards for calibration of Mn^{2+} and Fe^{3+} concentrations were prepared from ICP grade reagents.

2.4 Characterization

The morphology of as-grown products was investigated using transmission electron microscope (TEM, model MORGAGNI 268) operated at an accelerating voltage of 72 keV. The Nps subjected to TEM observations were dispersed in ethanol and drop-cast onto carbon-coated copper grid. Their average size was estimated from at least 150 species observed in the TEM images. High resolution transmission electron microscopy (HRTEM) studies were performed using a LIBRA 200 FE at an accelerating voltage of 200 keV.

X-ray powder diffraction experiments were performed on a D8 diffractometer (Bruker AXS, Germany), equipped with a Göbel mirror as a primary beam monochromator for CuK_α radiation. The average diameter (D) of Nps was calculated from the broadening of the XRD peak intensity using the Debye-Scherer equation, $D=k\lambda/\beta\cos\Theta$, where k is the Scherer factor (0.89), λ is the *X*-ray wavelength (0.154 nm) and β is the line broadening of a diffraction peak at angle Θ (Guinier *et al.* 1963).

Mössbauer spectra (MS) were collected in the transmission geometry from the spot of synthesized nanoparticles formed onto the shred of filter paper using Co^{57}(Rh) source. A closed cycle He cryostat (Advanced Research Systems, Inc.) was used for low temperature measurements. The hyperfine field B distributions and separate sextets or doublets were applied to fit the experimental spectra using WinNormos (Site, Dist) software. The hyperfine field value, B, decreased from the static maximum value, B_0, when the direction of magnetic moment of Nps fluctuates by small angle around magnetic easy axis, expressed by Eq. (1)

$$B = B_0\left(1-\frac{k_BT}{2KV}\right) \tag{1}$$

can be evaluated using a collective excitation model (Jones and Srivastava 1986). According to this theory, the amount of ΔB depends on the Np volume V, anisotropy energy constant K, and MS recording temperature T, where k_B is the Boltzmann constant. Upon increase in the MS recording temperature the direction of magnetic moment fluctuations becomes larger and in the case of uniaxial anisotropy, characteristic for $MnFe_2O_4$ Nps, the magnetic moment can change direction by 180°. In this case, the Neel superparamagnetic relaxation time given by

$$\tau = \tau_0\exp\left(\frac{KV}{k_BT}\right), \tag{2}$$

where τ_0 is the exponential pre-factor, decreases from 10^{-7} s to 10^{-9} s, whereas the sextets in Mössbauer spectra collapse to superparamagnetic singlet or doublet.

Magnetization measurements were accomplished using the vibrating sample magnetometer calibrated by Ni sample of similar dimensions as the studied sample. The magnetometer was composed of the vibrator, the lock-in-amplifier, and the electromagnet. The magnetic field was measured by the teslameter FH 54 (Magnet-Physics Dr. Steingrover GmbH).

3. Results and discussion

As the first step, manganese ferrite *Nps* were synthesized by autoclaving of alkaline solutions (pH≈12.0) containing only Mn(II) and Fe(III) sulfates at the 1:2 molar ratio, keeping the total concentration below 0.1 mol L^{-1}, at 120°C temperature for 5 to 15 h. In all cases, TEM images of the obtained products revealed *Nps*, which were non-uniform in shape and size (Fig. 1(b)). On the other hand, the XRD diffraction pattern of as-formed *Nps* (Fig. 1(a)) reveals eight relatively sharp peaks at 2Θ 18.02, 29.68, 35.00, 36.50, 42.48, 56.18 and 61.66 attributable to crystalline spinel

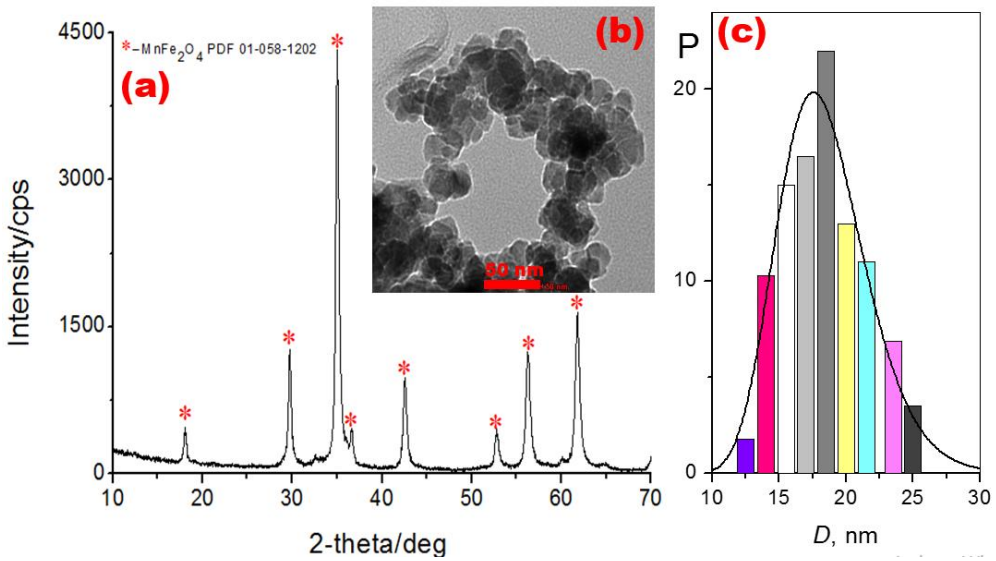

Fig. 1 Typical XRD pattern (a), TEM view (b) and size distribution histogram (c) of maganese ferrite nanoparticles fabricated by autoclaving an aqueous solution containing 40 $MnSO_4$+40 mmol L^{-1} $Fe_2(SO_4)_3$ +NaOH up to pH=12.2 at 120℃ for 10 h

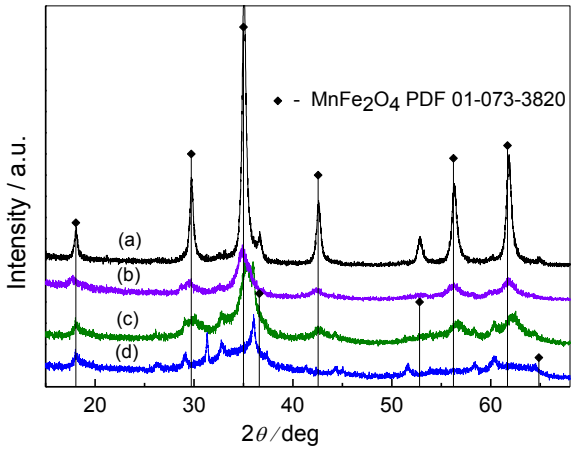

Fig. 2 XRD patterns of *Nps* synthesized in the solution containing 40 $MnSO_4$, 40 $Fe_2(SO_4)_3$ and 1.33 mmol L^{-1} PEG 3000 and NaOH up to pH: (a) 12.0, (b) 11.0, (c) 10.0, (d) 9.0 by autoclaving at 120 ℃ for 10 h

structure of jacobsite ($MnFe_2O_4$) with a cubic lattice and space group: Fd3m, *Z*=8, planes (111), (220), (311), (222), (400), (511) and (440), respectively, well corresponding with ICDD PDF 01-058-1202 data). Increase in the synthesis time up to 15 h had no influence on the phase composition of this product. Note, that quite similar results have been reported earlier for $MnFe_2O_4$ nanorods formation *via* surfactant-free hydrothermal route (Zheng *et al.* 2008). In the case of syntheses from more acidic or alkaline solutions, the additional diffraction peaks, besides those attributable to $MnFe_2O_4$, were detected indicating the formation of $MnCO_3$ (at pH=11.0) or $MnCO_3$, Fe_2O_3 and FeO(OH) (at pH=13.0) impurities together with $MnFe_2O_4$ (Fig. 2). These results indicated the crucial need for the addition of some structure-modifying agents to the synthesis reactor in order to obtain smaller and mono dispersed *Nps*. Therefore, in the next setup, the influence of various typical surfactants and complexants, particularly polyethylene and polypropylene glycols (PEG-3000 and PPG-425), citric and tartaric acids, their salts, glycine, cysteine, glucose, chitosan, etc. on the *Np* size, size distribution profiles, composition and yield were studied using various concentrations of these agents. Fig. 3 depicts the set of XRD patterns for the products synthesized under the same hydrothermal treatment conditions in alkaline solution containing Mn(II) and Fe(III) sulfate precursors at a 1:2 molar ratio and the same pH value but different *Np* growth modifying additives. As seen, the composition of the obtained products depends significantly on the nature of applied additive. Only in the case of PEG-3000 (Fig. 3(f)), triethanolamine (Fig. 3(g)) and PPG-425 (Fig. 3(h)) quite pure $MnFe_2O_4$ crystallites with average size of 12.5, 16.7 and 14.8 nm, respectively, were formed. In all of these cases, however, formation of some amount of Mn_3O_4 and FeO(OH) as impurities was also observed. On the other hand, the application of citric or tartaric acids and their sodium salts results in formation of nonmagnetic *Nps* composed mainly of Mn_3O_4 (PDF card no. 04-007-1841) (Fig. 3(a)). In the case of synthesis with amino acid cysteine, the main product was the mixture of sulfur and $Mn_3Fe_3O_8$ with some MnS inclusions (Fig. 3(c)). Similarly, only a mixture of nonstoichiometric manganese ferrite, MnO_2, Fe_2O_3, FeS and Mn° was formed under the same conditions when amino acid glycine was used in the hydrothermal reaction of Mn(II) and Fe(III) sulfates (Fig. 3(d)). It is also worth noticing that application of carbohydrates, such as glucose, sucrose and fructose lead to the formation of small $Mn_2Fe_3O_4$ crystallites mixed with magnetite and Mn_3O_4 (Fig. 3(c)).

The influence of each additive on the composition of *Nps* formed during the hydrothermal synthesis was found to be strongly dependent also on their concentration in the reaction medium. For example, quite pure crystalline $MnFe_2O_4$ *Nps* at approximately 98% yield were formed in the solutions containing up to 1.1 mmol L^{-1} PEG-3000. In the case of 1.33 mmol L^{-1} PEG content, however, the product obtained under the same conditions (pH = 12.0; 120 °C; 10 h) was composed of 97% jacobsite ($MnFe_2O_4$) with average 12.8 nm sized crystallite grains and 2.6% of twice larger-sized (23.9 nm) rhodochrosite ($MnCO_3$) crystals. When concentration of PEG was increased up to 10 mmol/L, the mixture of $MnFe_2O_4$ (42%) and $MnCO_3$ (58%) crystallites with smaller ferrite grains (9.15 nm) and slightly larger $MnCO_3$ grains (25 nm) was formed. At the same time, the pH of hydrothermal synthesis solutions also has a crucial influence on the purity and size of the synthesized products. From the XRD patterns (Fig. 2) of the products obtained under the same hydrothermal synthesis conditions, only in the medium with pH=12.0-12.5, pure $MnFe_2O_4$ crystallites were formed. Decrease in the pH value leads to the formation of smaller crystallites with various impurities. This fact points to the crucial need for determining the safe concentration of each applied additive at a given pH value.

Fig. 4 shows the magnetization (*m*) versus the applied magnetic field (*B*) plots recorded at room temperature for *Nps* synthesized under the same hydrothermal treatment conditions in the alkaline

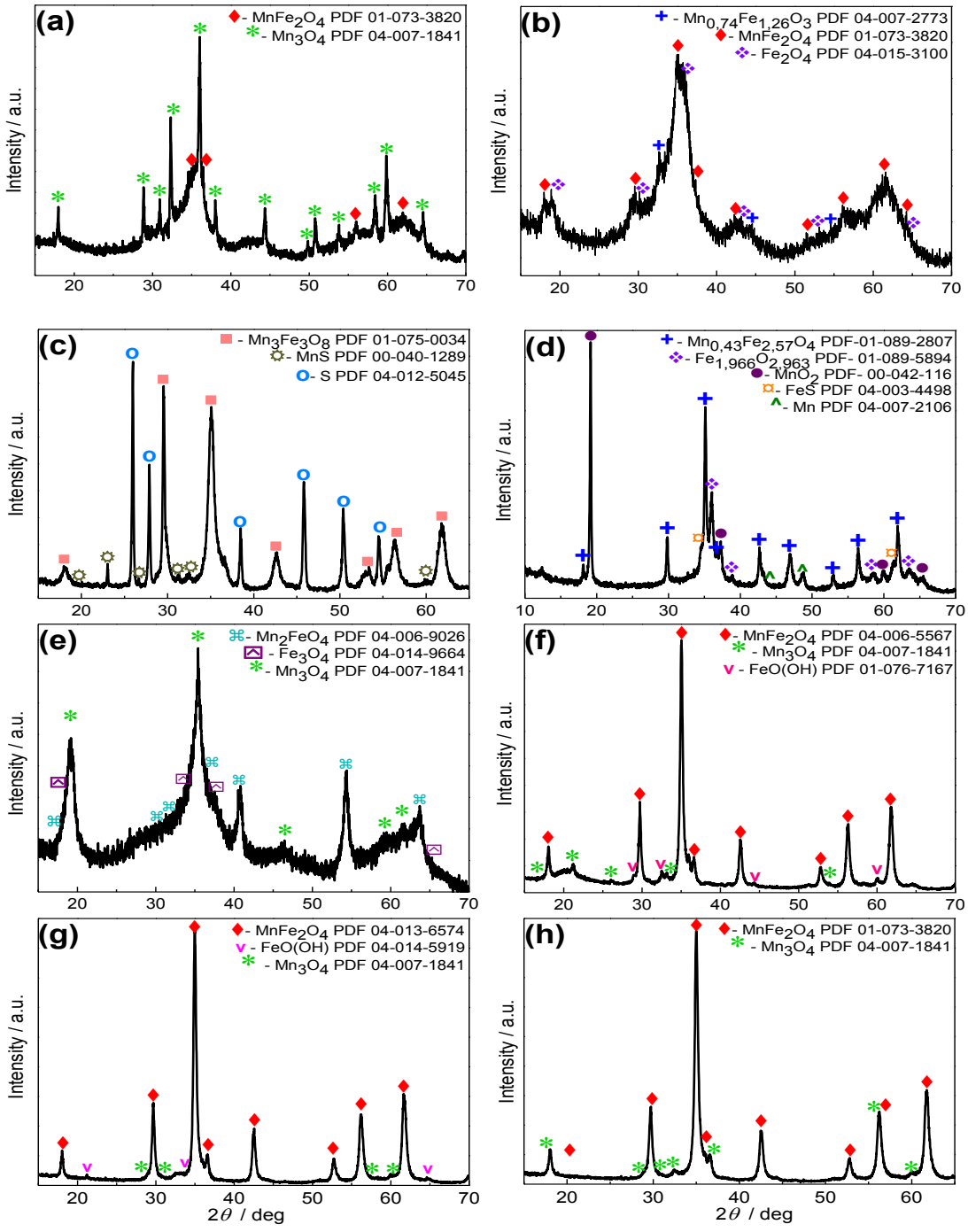

Fig. 3 XRD patterns of *Nps* synthesized in the solution containing 40 $MnSO_4$ and 40 mmol L^{-1} $Fe_2(SO_4)_3$ and: (a) 65 mmol L^{-1} citric acid, (b) 65 mmol L^{-1} K,Na tartrate, (c) 65 mmol L^{-1} cisteine, (d) 65 mmol L^{-1} glicine, (e) 22 mmol L^{-1} glucose, (f) 4.0 g L^{-1} chitosan, (g) 12 mmol L^{-1} TEA and (h) 1.33 mmol L^{-1} PEG 3000 by autoclaving at 120℃ for 10 h. pH 12.1-12.2

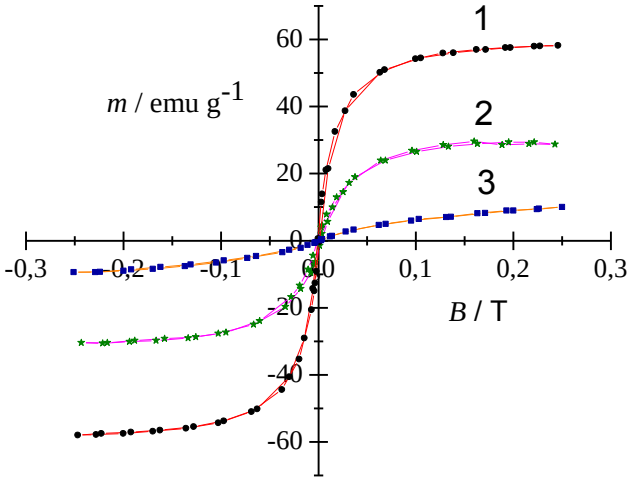

Fig. 4 Magnetization curves of *Nps* synthesized in the solutions containing 40 $MnSO_4$ + 40 mmol L^{-1} $Fe_2(SO_4)_3$ + NaOH up to pH 12.2 and: (1) 1.1 mmol L^{-1} PEG-3000; (2) 2.6 mmol L^{-1}chitosan; (3) 65 mmol .L^{-1} citric acid by autoclaving at 120°C for 10 h

$MnSO_4$ and $Fe_2(SO_4)_3$ solution containing three most frequently used chelating ligands, which are known to influence reactivity of the co-precipitation reaction precursors, i.e., polyethylene glycol, chitosan and citric acid (Hubert-Pfalzgraf 1998, Hu *et al*.2007, Byrappa *et al*. 2008). It can be inferred from the hysteresis loops that all these *Nps* are superparamagnetic at room.temperature although their magnetic properties differ significantly. The saturation magnetization of *Nps*, fabricated in the PEG- 3000, chitosan and citric acid containing solutions was found to be about 61, 33 and 4 emu g^{-1}, respectively. Although lower than for bulk $MnFe_2O_4$ material (80 emu/g) (Brabers 1995), quite high saturation magnetization value of PEG-functionalized $MnFe_2O_4$ *Nps* should be linked with their quite single crystallographic phase, corresponding to jacobsite with a cubic lattice, where *a*=8.4906(7) Å, and crystallite size of 14±0.5 nm, what was determined by Scherer approach and confirmed by TEM observations. It is worth noticing that addition of PEG to the reaction solution resulted in the formation of significantly smaller and monodisperser *Nps* possessing high crystallinity with *d*=2.99 Å lattice fringes, close to typical *d*=3.00 Å in a (220) plane of $MnFe_2O_4$ (Fig. 5(b)), whereas (111) planes are more typical for *Nps* synthesized in the same solution without PEG (Fig. 5(a)).

Without any doubt, weak ferromagnetic behavior of *Nps* synthesized in the citric acid containing medium should be attributed to the fact that main component of these *Nps* is Mn_2O_3 (Fig. 3(a)). Moreover, according to the TEM observations, XRD and Mössbauer spectra (not shown herein), the size of these *Nps* is smaller than 5 nm. In the case of hydrothermal synthesis in the chitosan-containing solution, $MnFe_2O_4$ *Nps* contained some quantity of Mn_2O_3 and FeOOH impurities (Fig. 3(f)). Therefore, twice lower saturation magnetization value of these *Nps* could also be ascribed to poor $MnFe_2O_4$ *Nps* crystal structure as well as purity, since even small content of weakly magnetic impurities can significantly reduce their saturation magnetization value (Laokul *et al*. 2011, Naseri *et al*. 2012). Therefore we note that there are many factors related to the decomposition of additives in the reaction medium, which can be important in the hydrothermal synthesis of $MnFe_2O_4$ *Nps*, but it is difficult to take them into our consideration

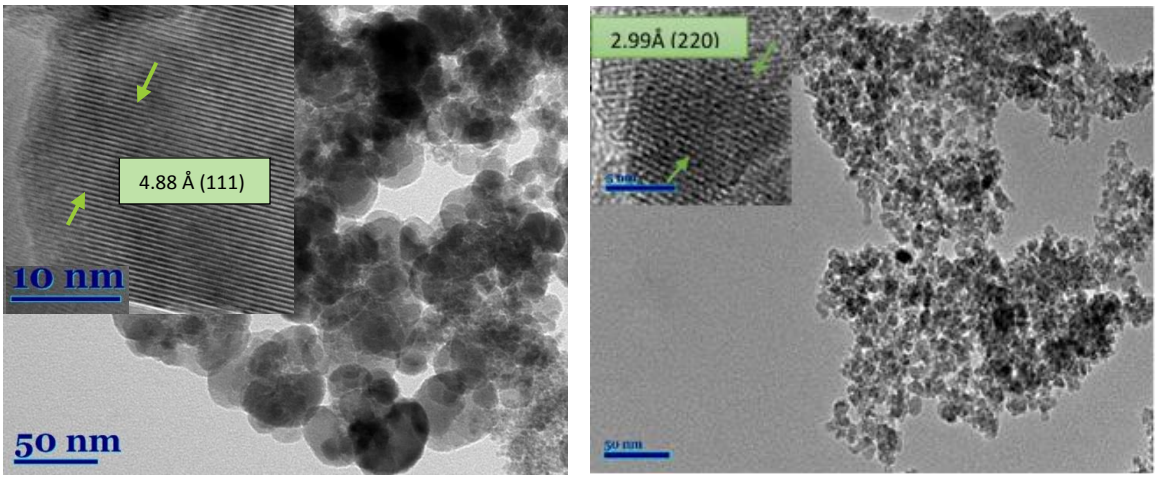

(a) (b)

Fig. 5 SEM and HRTEM (Insets) images of nanoparticulated species synthesized by hydrothermal treatment in the solution containing 25 $MnSO_4$ +25 mmol/L $Fe_2(SO_4)_3$ + NaOH up to pH=12,04 (a) and in the same solution containing additionally 1.1 mmol L^{-1} PEG-3000 (b) at 120℃ for 10 h

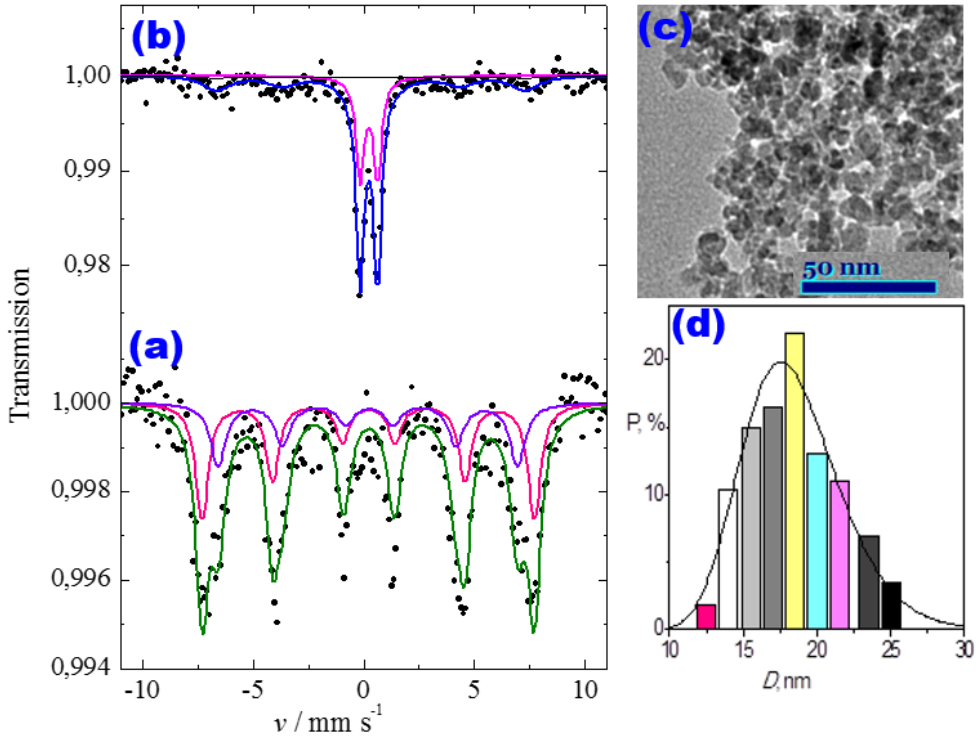

Fig. 6 Room temperature transmission Mössbauer spectra (a, b) and TEM view (c) for $MnFe_2O_4$ *Nps* synthesized hydrothermally in the alkaline (pH=12.25) solution containing 50 $MnSO_4$ and 50 mmol L^{-1} $Fe_2(SO_4)_3$ and NaOH without (a) or containing additionally 65 mmol L^{-1} glycine (b) or 4.0 mmol L^{-1} PPG (c) at 120℃ for 10 h. The size distribution hystogram of *Nps* fabricated under (c) conditions are shown in (d)

without more detailed investigations of each case. For example, Fig. 6 depicts the Mössbauer spectra of manganese ferrite *Nps* synthesized in the glycine-containing (b) and PEG-3000-containing (a) solutions under the same conditions. As seen, the Mössbauer spectrum (MS) of glycine-funcionalized *Nps* is doublet-shaped which is common characteristic of *Nps* less than 5 nm in size (SEM image in Fig. 5) (Liu *et al*. 2009, Peddis *et al*. 2008). At the same time, some tested additives such as PPG were ineffective for the size and size distribution range of $MnFe_2O_4$ *Nps* synthesized under hydrothermal conditions, as these parameters remained very similar to those of *Nps* formed without structure-modifying agents (Fig. 6(c)). Consequently, MS sextet characteristic of *Nps* larger than 10 nm is observed for all these ferrites (Fig. 6(a)). Two sextets of different splitting (hyperfine field B=42, 46.6 T) and same isomer shift (0.32 mm/s) in Fig. 6(a) represent influence of size distribution to hyperfine field (Eq. (1)). Likewise, low intensity sextet aside doublet (Fig. 6(b)) arises due to the part of larger nanoparticles.

Based on the results obtained by XRD, TEM and XRD, it can be concluded that application of most traditional chelating and complexing additives is not suitable for predictable synthesis of $MnFe_2O_4$ *Nps* from the sulfate precursors by hydrothermal approach. Quite similar results were also obtained by hydrothermal synthesis of $MnFe_2O_4$ *Nps* in the alkaline solution composed of Mn(II) and Fe(III) chloride precursors. In this case, however, pure crystalline manganese ferrite *Nps* are formed in slightly lower pH region centered in the vicinity of 11.5±0.5 (Fig. 7). Decrease in pH of the tested solutions to 10.5 and below resulted in the formation of $MnFe_2O_4$ and $MnCO_3$ mixed composition crystals (Fig. 7(a-2)), whereas increase in pH above 12.0 led to the formation of FeO(OH), Fe_2O_3 and Mn_2O_3 impurities, along with $MnFe_2O_4$ (Fig. 7(b)). It is worth noticing, however, that even at the optimal Mn(II) and Fe(III) chlorides concentrations (molar ratio 1:2), pH=11.5, and hydrothermal synthesis conditions (120℃), the as-formed pure $MnFe_2O_4$ crystallites varied in the size from several to 25 nm and were prone to agglomerate.

Fig. 8 demonstrates the effect of various additives on the composition of nanoparticulated species fabricated by hydrothermal synthesis in the chloride solutions kept at the optimal pH value of 11.5. As seen from the XRD patterns, quite pure $MnFe_2O_4$ *Nps* were formed only in the glycine

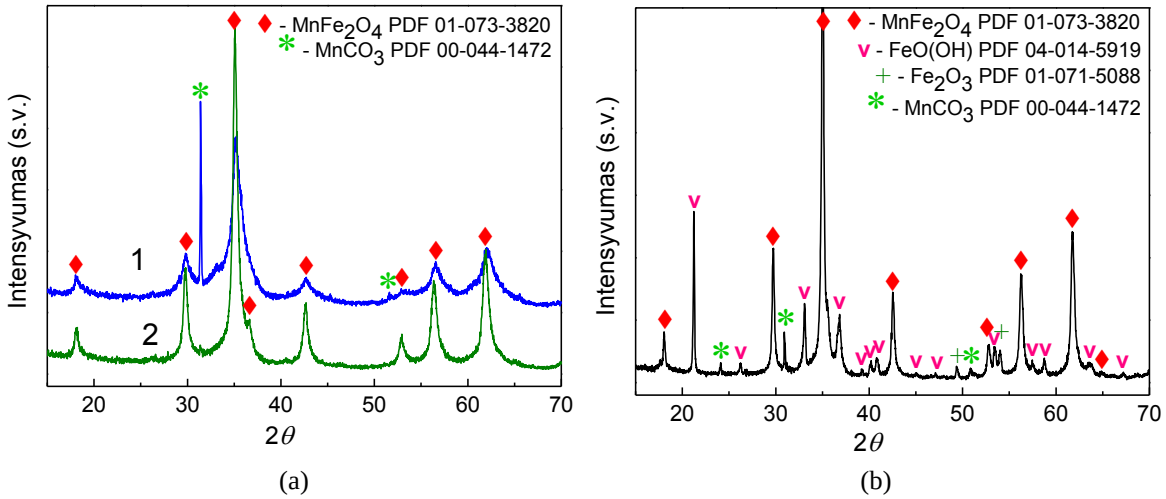

Fig. 7 XRD patterns of *Nps* synthesized from 25 $MnCl_2$ + 50 mmol L^{-1} $FeCl_3$ + NaOH solution up to pH: 10,5 (a-1), 11,5 (a-2) ir 12,2 (b) by hydrotheral treatment at 120℃ for 10 h

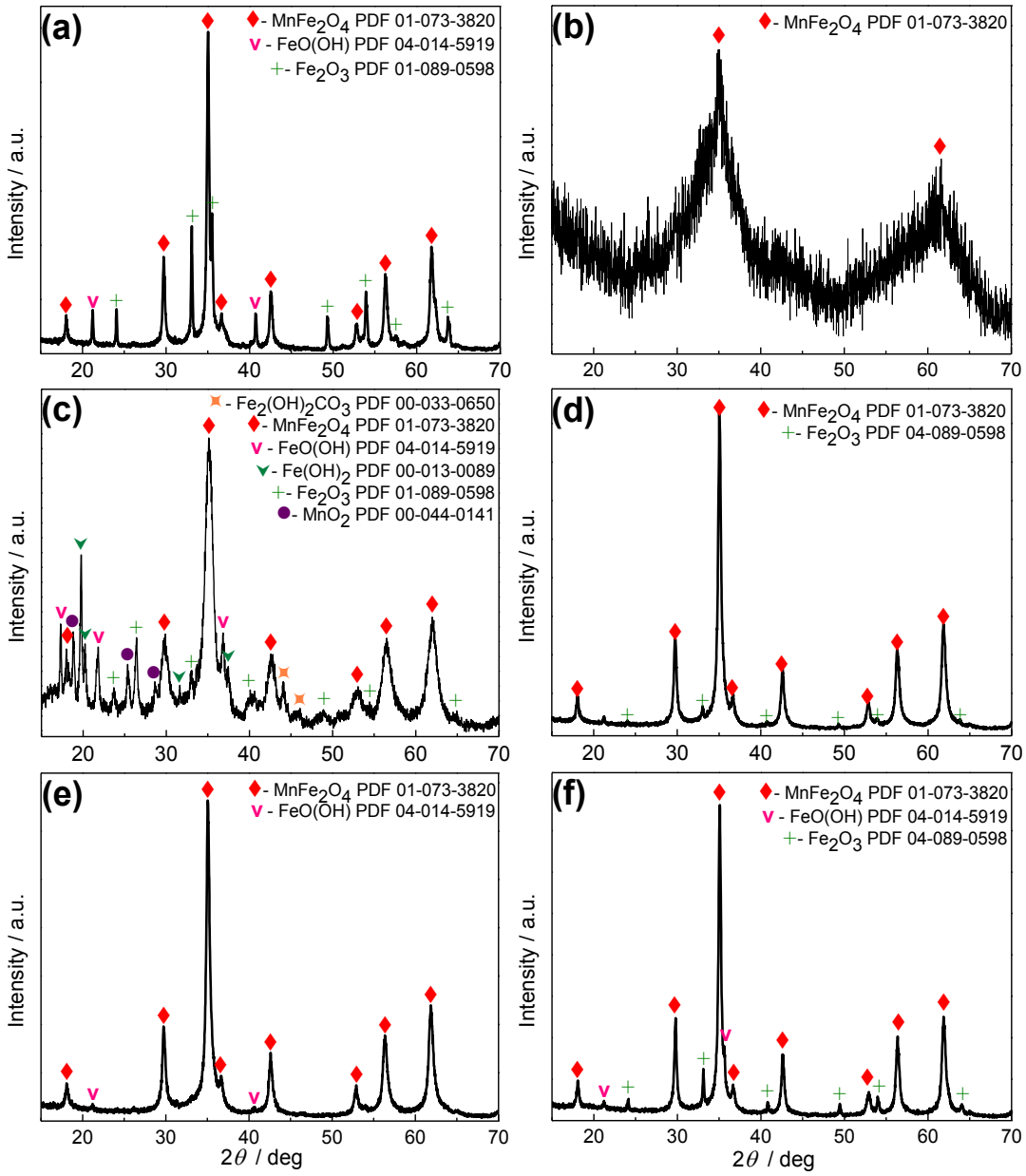

Fig. 8 XRD patterms of the products synthesized in 25 $MnCl_2$ and 50 mmol/L $FeCl_3$ solutions containing 4.0 mmol L^{-1} PPG 425 (a), 65 mmol L^{-1} potassium sodium tartrate (b), 65 mmol L^{-1} cysteine (c), 65 mmol L^{-1} glycine (d), 1.33 mmol L^{-1} PEG 3000 (e) and 4.0 g L^{-1} chitosan (f) at pH=11.5 by hydrothermal treatment at 120℃ for 10h

(97.5%) and PEG-3000 (98.3%) containing solutions (Fig. 8(d) and (e), respectively) implying on their prospective future application.

3. Conclusions

It was determined that the majority of tested chelating and Me^{z+} complexing additives, besides the expected control of the particle size and size dispersity, also have a strong effect on the purity of the product obtained by hydrothermal as well as microwave-assisted synthesis by co-precipitation reaction

$$Mn^{2+} + 2Fe^{3+} + 8OH^- \rightarrow MnFe_2O_4 + 4H_2O, \quad (3)$$

characteristic to the formation of ferrites in the alkaline solutions. Therefore, the application of such additives as cysteine, glycine, citric and tartaric acid and their salts for the synthesis of pure phase $MnFe_2O_4$ nanoparticles is not suitable. On the other hand, the influence of the tested three additives, such as PPG, PEG and chitosan, on the purity of the synthesized *Nps* is significantly weaker, therefore they can be used for the production of superparamagnetic $MnFe_2O_4$ *Nps* with a good yield. However, to clarify in detail the reasons of the parasitic impurities formation along with $MnFe_2O_4$ additional investigations should be conducted for each case that was beyone the scope of this study.

Acknowledgements

Dr. J. Vaičiūnienė is gratefully acknowledged for performing the analysis of solutions. Authors are also grateful to Dr. R. Kondrotas for obtaining TEM images.

References

Ahn, T., Kim, J.H., Yang, H.M., Lee, J.W. and Kim, J.D. (2012), "Formation pathways of magnetite nanoparticles by coprecipitation method", *J. Phys. Chem. C*, **116**, 6069-6076.

Banerjee, S.S. and Chen, D.H. (2008), "Multifunctional pH-sensitive magnetic nanoparticles for simultaneous imaging, sensing and targeted intracellular anticancer drug delivery", *Nanotechnology*, **19**, 505104.

Bao, N., Shen, L., An, W., Padhan, P., Turner, C. and Gupta, A. (2009), "Formation mechanism and shape control of monodisperse magnetic $CoFe_2O_4$ nanocrystals", *Chem. Mater*., **21**(14), 3458-3468.

Brabers, V.A.M. (1995), *Progress in spinel ferrite research*, Handbook of Magnetic Materials, Ed. Buschow, K.H.J., Vol. 8, Chapter 3, Elsevier, NY, USA.

Byrappa, K., Ohara, S. and Adschiri, T. (2008), "Nanoparticles synthesis using supercritical fluid technology-towards biomedical applications", *Adv. Drug, Delivery Rev*., **126**, 273-279.

Coker, V.S., Telling, N.D., van der Laan, G., Pattrick, R.A.D., Pearce, C.I., Arenholz, E., Tuna, F., Winpenny, R.E.P. and Lloyd, J.R. (2009), "Harnessing the extracellular bacterial production of nanoscale cobalt ferrite with exploitable magnetic properties", *ACS Nano*, **3**(7), 1922-1928.

Corchero, J. and Villaverde, A. (2009), "Biomedical applications of distally controlled magnetic nanoparticles", *Trend. Biotechnol*., **27**(8), 468-476.

Guinier, A., Lorrain, P. and Lorrain, D.S.M. (1963), *X-Ray Diffraction : In Crystals, Imperfect Crystals and Amorphous Bodies*, Freeman, W.H. & Co., San Francisco, CA, USA.

Gupta, A.K. and Gupta, M. (2005), "Synthesis and surface engineering of iron oxide nanoparticles for biomedical applications", *Biomater*., **26**, 3995-4021.

Hu, Y., Xie, W., Tang, Y.W. and Wan, C.H. (2007), "Effect of PEG conformation and particle size on the cellular uptake efficiency of nanoparticles with the HepG2 cells", *J. Controll. Relase*., **118**, 7-17.

Hubert-Pfalzgraf, L.G. (1998), "Some aspects of homo and heterometallic alkoxides based on functional alcohols", *Coordinat. Chem. Rev*., **178-180**, 967-997.

Janghorban, K. and Shokrollahi, H. (2007), "Influence of V_2O_5 addition on the grain growth and magnetic properties of Mn-Zn high permeability ferrites", *J. Magn. Magn. Mater*., **308**, 238-242.

Jiang, J.Z., Wynn, S., Morup, S., Okada, T. and Berry, F.J. (1999), "Magnetic structure evolution in mechanically milled nanostructured $ZnFe_2O_4$ particles", *Nanostruct. Mater.*, **12**, 737-74.

Jones, D.H. and Srivastava, K.K.P. (1986), "Many-state relaxation model for the Mossbauer spectra of superparamagnets", *Phys. Rev. B*, **34**, 7542-7548.

Kumar, C.S.S.R. and Mohammad, F. (2011), "Magnetic nanoparticles for hyperthermia-based therapy and controlled drug delivery", *Adv. Drug. Delivery Rev*., **6 3**, 789-808.

Latrigue, L., Wilhelm, C., Servais, J., Factor, R., Dencousse, A., Bacri, J.C., Luciani, N. and Gazeau, F. (2012), "Nanomagnetic Sensing of Blood Plasma Protein Interactions with Iron Oxide Nanoparticles: Impact on Macrophage Uptake", *ACS Nano*, **6**, 2665 - 2678.

Laokul, P., Amornkitbamrung, V., Seraphin, S. and Maensiri, S. (2011), "Characterization of magnetic properties of nanocrystalline $CuFe_2O_4$, $NiFe_2O_4$, $ZnFe_2O_4$ powders prepared by the Aloe vera extract solution", *Curr.Appl. Phys.*, **11**(1), 101-108.

Laurent, S., Forge, D., Port, M., Roch, A., Robic, C., Elst, L.V. and Muller, R.N. (2008), "Magnetic iron oxide nanoparticles: synthesis, stabilization, vectorization, physicochemical characterizations, and biological applications", *Chem. Rev*., **108**, 2064-2110.

Lee, D.K., Kim, Y.H., Kang, Y.S. and Stroeve, P. (2005), "Preparation of a Vast $CoFe_2O_4$ Magnetic Monolayer by Langmuir-Blodgett Technique", *J. Phys. Chem. B*, **109**(31), 14939-14944.

Liu, B.H., Ding, J., Dong, Z.L., Boothroyd, C.B., Yin, J.H. and Yi, J.B. (2006), "Microstructural evolution and its influence on the magnetic properties of $CoFe_2O_4$ powders during mechanical milling", *Phys. Rev. B*, **74**, 184427.

Liu, Y., Zhang, Y., Feng, J.D., Li, C.F., Shi, J. and Xiong, R. (2009), "Dependence of magnetic properties on crystallite size of $CoFe_2O_4$ nanoparticles synthesised by auto-combustion method", *J. Exp. Nanosci*., **4**, 159-168.

Lu, A.H., Salabas, E.L. and Schuth, F. (2007), "Magnetic Nanoparticles: Synthesis, Protection, Functionalization, and Application", *Angew. Chem. Int. Ed*., **46**, 1222-1244.

Mahmoudi, M., Sant, S., Wang, B., Laurent, S. and Sen, T. (2011), "Superparamagnetic iron oxide nanoparticles (SPION's): Development, surface modification and application in chemotherapy", *Adv. Drug Delivery Rev*., **63**, 24-46.

Naseri, M.G., Saion, E.B. and Kamali, A. (2012), "An overview on nanocrystalline $ZnFe_2O_4$, $MnFe_2O_4$, and $CoFe_2O_4$ synthesized by a thermal treatment method", *ISRN Nanotechnol.*, ID 604241, doi:10.5402/2012/604241.

Peddis, D., Cannas, C., Musinu, A. and Piccaluga, G. (2008), "Coexistence of superparmagnetism and spin-glass like magnetic ordering phenomena in a $CoFe_2O_4$-SiO_2 nanocomposite", *J. Phys. Chem. C*, **112**(13), 5141-5147.

Pereira, C., Pereira, A.M., Fernandes, C., Araujo, J.A., Freire, C. *et al* (2012), "Superparamagnetic $MeFe_2O_4$ (M=Fe, Co, Mn) nanoparticles: tuning the particle size and magnetic properties through a novel one-step coprecipitation route", *Chem. Mater.*, **24**, 1496-1504.

Pramanik, N.C., Fujii, T., Nakanishi, M. and Takada, J. (2004), "Effect of Co^{2+} ion on the magnetic properties of sol-gel cobalt ferrite thin films", *J. Mater. Chem*., **14**, 3328-3332.

Pratsinis, S.E. and Vemury, S. (1996), "Particle formation in gases-a review", *Powder Technol*., **88**, 267-272.

Salazar, J.S., Perez, L., de Abril, O., Phuoc, L.T., Ihiawakrim, D., Vazgues, M., Greneche, J.M., Begin-Colin, S. and Pourroy, G. (2011), "Magnetic Iron Oxide Nanoparticles in 10-40 nm Range: Composition in terms of magnetite/maghemite ratio and effect on the magnetic properties", *Chem. Mater. B*, **23**, 1379-1386.

Shokrollahi, H. (2008), "Magnetic properties and densification of manganese-zinc soft ferrites ($Mn_{1-x}Zn_xFe_2O_4$) doped with low melting point oxides", *J. Magn. Magn. Mater*., **320**, 463-474.

Solano, E., Perez-Mirabet, L., Martinez-Julian, F., Guzman, R., Arbiol, J. *et al.* (2012), "Facile and efficient one-pot solvothermal and microwave-assisted synthesis of stable colloidal solutions of MFe_2O_4 spinel magnetic nanoparticles", *J. Nanopart. Res*., **14**, 1034-1038.

Sun, S., Zeng, H., Robinson, D.B., Raoux, S., Rice, P.M., Wang, S.X. and Li, G. (2004), "Monodisperse MFe_2O_4 (M=Fe, Co, Mn) nanoparticles", *J. Am. Chem. Soc*., **126**(1), 273-279.

Thomas, M.F. and Johnson, C.E. (1986), "Mössbauer spectroscopy", Dickson D.P.E. and Berry F.J. Cambridge University Press, Cambridge.

Tourinho, F.A., Franck, R. and Massart, R. (1990), "Aqueous ferro fluids based on manganese and cobalt ferrites", *J. Mater. Sci*., **25**, 3249-3254.

Yang, H., Zhang, C., Shi, X., Hu, H., Du, X., Fang, Y., Ma, Y., Wu, H. and Yang, S. (2010), "Water-soluble super paramagnetic manganese ferrite nanoparticles for magnetic resonance imaging", *Biomater*., **31**, 3667-3673.

Zeng, H., RiCe, P.M., Wang, S.X. and Sun, S. (2004), "Monodisperse MFe_2O_4 (M=Fe,Co,Mn) nanoparticles", *J. Am. Chem. Soc*., **126**, 11458-11459.

Zheng, L., He, K., Xu, C.Y. and Shao, W.Z. (2008), "Synthesis and characterization of single crystalline $MnFe_2O_4$ nanorods via a surfactant-free hydrothermal route", *J. Magn. Magn. Mater*., **320**(21), 2672-2675.

CC